ΛCDM or self-interacting neutrinos: How CMB data can tell the two models apart

Minsu Park,[1,2,*] Christina D. Kreisch,[2,†] Jo Dunkley,[1,2] Boryana Hadzhiyska,[3] and Francis-Yan Cyr-Racine[3,4]

[1]Department of Physics, Princeton University, Princeton, New Jersey 08544, USA
[2]Department of Astrophysical Sciences, Princeton University, Princeton, New Jersey 08544, USA
[3]Department of Physics, Harvard University, Cambridge, Massachusetts 02138, USA
[4]Department of Physics and Astronomy, University of New Mexico, 1919 Lomas Boulevard NE, Albuquerque, New Mexico 87131, USA

(Received 24 April 2019; published 20 September 2019)

Of the many proposed extensions to the ΛCDM paradigm, a model in which neutrinos self-interact until close to the epoch of matter-radiation equality has been shown to provide a good fit to current cosmic microwave background (CMB) data, while at the same time alleviating tensions with late-time measurements of the expansion rate and matter fluctuation amplitude. Interestingly, CMB fits to this model either pick out a specific large value of the neutrino interaction strength, or are consistent with the extremely weak neutrino interaction found in ΛCDM, resulting in a bimodal posterior distribution for the neutrino self-interaction cross section. In this paper, we explore why current cosmological data select this particular large neutrino self-interaction strength, and by consequence, disfavor intermediate values of the self-interaction cross section. We show how it is the $\ell \gtrsim 1000$ CMB temperature anisotropies, most recently measured by the *Planck* satellite, that produce this bimodality. We also establish that smaller scale temperature data, and improved polarization data measuring the temperature-polarization cross-correlation, will best constrain the neutrino self-interaction strength. We forecast that the upcoming Simons Observatory should be capable of distinguishing between the models.

DOI: 10.1103/PhysRevD.100.063524

I. INTRODUCTION

Within the Standard Model of particle physics, neutrinos remain elusive. While universally present, their weak interactions with other particles make them difficult to study directly. Neutrino oscillation experiments have shown that neutrinos have mass [1,2], but the Standard Model does not account for the mechanism that generates this mass [3–6]. This presents the neutrino sector as an intriguing source of new physics.

In the Standard Model we assume neutrinos interact only through the electroweak interaction and decouple from the cosmic plasma at a temperature of 1.5 MeV [7]. Once decoupled, the neutrinos freely streamed through the early Universe, interacting only through gravity. The free-streaming of these gravitationally coupled neutrinos imposes a shear stress on the matter as it streams past, damping acoustic oscillations in the photon-baryon plasma and boosting CDM fluctuations at horizon entry [8]. Recent observations of the cosmic microwave background (CMB), most recently by the *Planck* collaboration [9] using TT, TE, EE + lowE + lensing + BAO data, have put bounds on neutrino parameters, including the effective number of neutrino species ($N_{\rm eff} = 2.99^{+0.34}_{-0.33}$) and the sum of the species' masses ($\sum m_\nu < 0.12$ eV). The $N_{\rm eff}$ measurement is consistent with the theoretical prediction of 3.046 [10]. The $\sum m_\nu$ measurement is approaching the lower mass limit for the inverted neutrino hierarchy, $\sum m_\nu \geq 0.1$ eV, from neutrino oscillation experiments [1,2]. Cosmological data can now put competitive constraints on neutrino physics.

New neutrino interactions have become a topic of increasing interest due their impact on cosmological observables via altering neutrino free-streaming during the radiation dominated era (see e.g., Refs. [11–44]). Past studies [45–50] have explored the viability of stronger neutrino self-scattering, using a Yukawa interaction model parametrized by an interaction strength, $G_{\rm eff}$. Here the rate of scattering, Γ_ν, scales as $\Gamma_\nu \propto G_{\rm eff}^2 T_\nu^5$ where T_ν is the temperature of the cosmic neutrino background [45–49]. With increased $G_{\rm eff}$, neutrino-neutrino coupling is stronger in the early Universe. While neutrinos would still decouple from the rest of the plasma at 1.5 MeV, the stronger neutrino-neutrino coupling ultimately delays neutrino free-streaming to epochs of lower energies and so lower redshifts.

A delay in the onset of neutrino free-streaming affects the amplitude and phases of the CMB power spectrum (see [46,51] for more details.). A model with a nonzero value of

*minsup@princeton.edu
†ckreisch@astro.princeton.edu

$G_{\rm eff}$ has been shown to fit current cosmological data and produce a bimodal posterior probability for the interaction rate: a weak mode with low self-scattering strength $G_{\rm eff}$, essentially indistinguishable from no self-scattering (ΛCDM), and a strong self-interacting mode with $G_{\rm eff}$ of order 10^{-2} MeV^{-2}, where the neutrinos start free streaming at neutrino temperatures as low as 25 eV [45–47]. The strong mode is particularly interesting as it has a larger predicted Hubble constant [52] than the usual ΛCDM model, and a lower predicted amplitude of structure [53], which are preferred by other astronomical datasets.

In this paper we further explore which aspects of current CMB data produce the degeneracy between the two models. We identify the part of the *Planck* data responsible for producing the bimodality, which was not present with the WMAP data, and show how the data exclude models with moderate self-interaction. We then assess how upcoming CMB data might distinguish between the two models. This extends similar investigations in [47].

II. METHODS

We use Markov Chain Monte Carlo methods to map out the posterior distribution for a nine-parameter cosmological model: six parameters are the usual ΛCDM parameters (baryon density, cold dark matter density, angular peak position, spectral index and amplitude, and optical depth) and we also vary the effective number of neutrino species, $N_{\rm eff}$, the sum of neutrino masses, $\sum m_\nu$, and the interaction strength $G_{\rm eff}$. We impose linear priors on all parameters, except $G_{\rm eff}$ which takes a logarithmic prior. This prior choice is further discussed in Sec. III A. We use the CosmoMC sampling code [54] with Multinest [55], which is well suited to multimodal posteriors. We use the same modified Boltzmann code, CAMB, as in [46], and implement the same modifications in the CLASS code as a cross-check.

The datasets used are *Planck* 2015 temperature and lensing likelihood using the PLIK-LITE code [56,57], combined with current baryon acoustic oscillation (BAO) data [58–60], and a Gaussian prior on the optical depth of $\tau = 0.058 \pm 0.012$ from *Planck*. We also examine the effect of replacing just the *Planck* TT data with the WMAP nine-year TT and TE data [61], using the same BAO data and optical depth prior. Additionally, we generate simulated TT, TE and EE spectra representative of the upcoming Simons Observatory (SO), with co-added white noise levels of 5 μK-amin over 40% of the sky, a 1.4′ beam and maximum multipoles of $\ell = 3000$ in temperature and $\ell = 5000$ in polarization [62].[1] We describe the input models for these simulations in Sec. III C.

[1]In this study we do not include the nonwhite noise and residual foregrounds considered in [62].

III. RESULTS

A. Parameter distributions with current data

In Fig. 1 we show a set of the posterior distributions for the sampled and derived parameters for the *Planck* data compared to the WMAP data. Both datasets were accompanied by the same BAO data and τ prior. For *Planck* we find results consistent with [46,47], with a bimodal distribution for $G_{\rm eff}$. One mode is consistent with ΛCDM, and the other strong mode has nonzero interactions. We identify the preferred parameters for each mode by plotting them separately in Fig. 1, in addition to the joint distribution. The weak mode has $\log_{10}(G_{\rm eff}{\rm MeV}^2) < -3.04$, $\sum m_\nu < 0.2$ eV, and $N_{\rm eff} = 3.19^{+0.51}_{-0.48}$ at 95% CL whereas the strong mode prefers $\log_{10}(G_{\rm eff}{\rm MeV}^2) = -1.36^{+0.24}_{-0.30}$ and has $\sum m_\nu = 0.30^{+0.26}_{-0.25}$ eV, $N_{\rm eff} = 3.80^{+0.78}_{-1.0}$ at 95% CL. The strong mode also has a higher Hubble constant, a smaller comoving sound horizon at baryon drag epoch, $r_{\rm drag}$, and a lower amplitude of the matter power spectrum, σ_8. These parameter differences compensate for the introduction of the nonzero $G_{\rm eff}$. The strong mode gives a better consistency between *Planck* and WMAP in their best fitting H_0 and $r_{\rm drag}$ posteriors which is desirable.

It is important to consider how much the choice of prior impacts the parameters. The posterior for the strongly self-interacting neutrinos is enhanced if we impose a linear prior on $G_{\rm eff}$, as the density of points probed is higher around the region where $G_{\rm eff}$ is nonzero. For our logarithmic prior, the parameter volume of an interacting scenario is relatively smaller. For our analysis, we chose a logarithmic prior as it does not make an explicit choice for the energy scale of the problem [45].

When using the WMAP data, which measures angular multipoles $\ell \leq 1200$, we find in Fig. 1 that the distribution is not bimodal. Instead, the neutrino self-interaction strength is consistent with zero and has an upper limit of $\log_{10}(G_{\rm eff}{\rm MeV}^2) < -1.85$ at 95% confidence. It is only when using smaller-scale data, with $\ell > 1000$, that the bimodality appears. Indeed, this bimodality was first found when combining WMAP data with data from the Atacama Cosmology Telescope and South Pole Telescope small-scale CMB experiments [45]. Figure 1 also shows that the WMAP data do not favor the strongly interacting mode, implying that the smaller scale data in the $1200 < \ell \leq 2500$ range enhance the preference for the strong mode.

B. CMB spectra as a function of increasing $G_{\rm eff}$

To understand why the two models fit both datasets well, and why the central region with $G_{\rm eff} \approx 10^{-2.5}$ MeV^2 is excluded by the *Planck* data, we identify best-fitting models in each of the two peaks of the distribution: one with no, or low, self-interaction (essentially ΛCDM), and the other with high self-interaction strength. Sampling

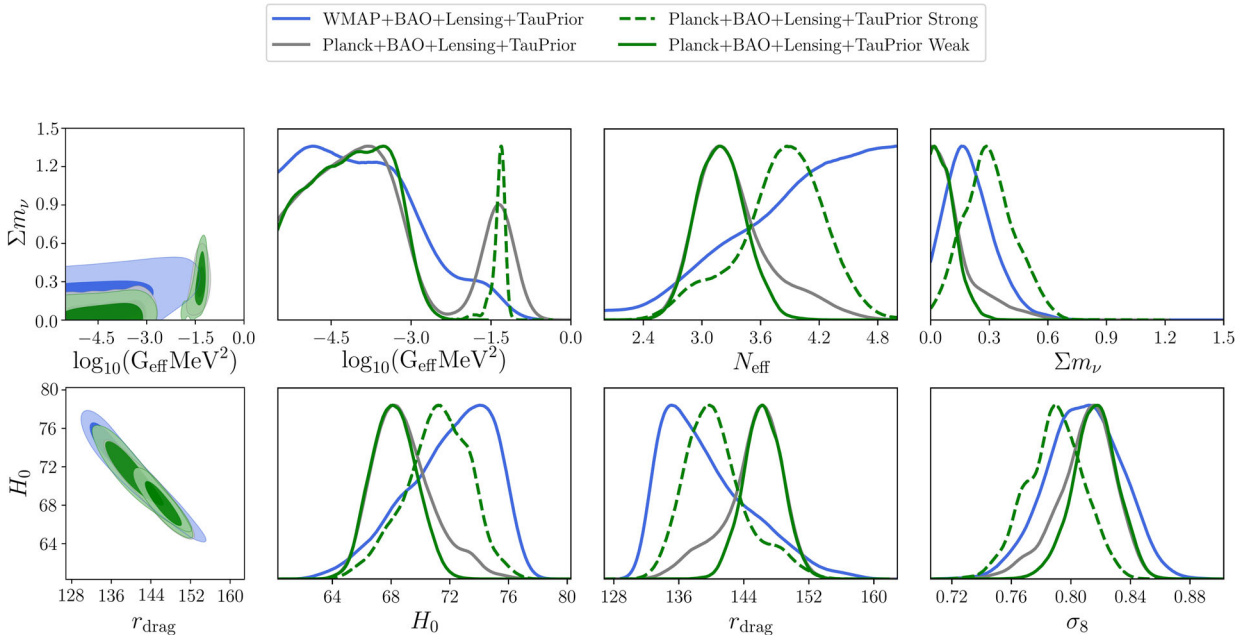

FIG. 1. Probability distributions for parameters from a nine-parameter model (ΛCDM plus neutrino self-interaction strength $G_{\rm eff}$, effective neutrino number, and neutrino mass), using the WMAP and *Planck* CMB data combined with BAO and *Planck* lensing data. The parameters derived using *Planck* are consistent with previous results [46] and show the clear bimodality in the neutrino self-interaction strength. The $\sum m_\nu$ and $\log_{10}(G_{\rm eff}{\rm MeV}^2)$ posteriors hit the lower ends of their priors, 0 and −5.5 respectively. At the −5.5 lower end the model is very close to ΛCDM. The "strong" and "weak" distributions show the marginalized posteriors when considering each of the bimodal islands separately. For the unseparated distribution, the strong mode has a lower marginalized posterior relative to the weak mode. The distribution using just WMAP data is not bimodal.

evenly spaced points along the straight line connecting the peaks in the nine-dimensional parameter space, as shown in Fig. 2, we compute the likelihood of each of the datasets, and generate the CMB power spectra corresponding to each point.

Figure 3 shows the *Planck* PLIK-LITE $-\chi^2$ $(= 2\ln\mathcal{L})$ along this path. We find that the two modes are each similarly well fitted to the data, with $\chi^2_{\rm strong} - \chi^2_{\rm weak} \approx 6$ but there exists a valley of bad fitting in between them.

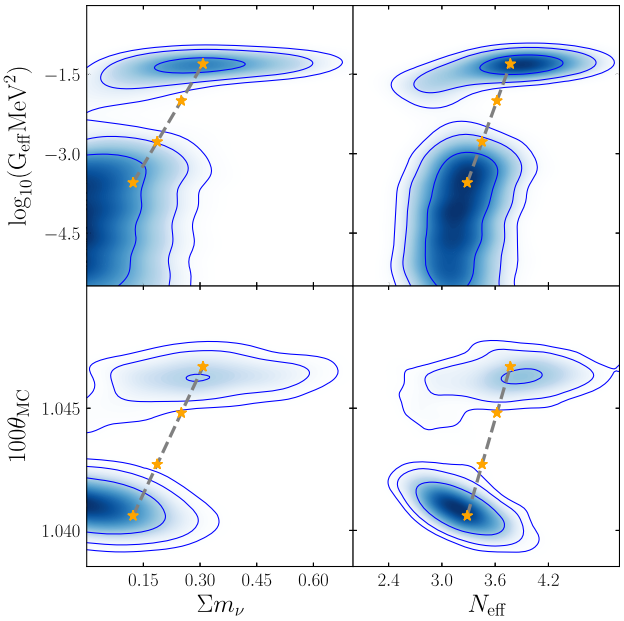

FIG. 2. Illustration of the line connecting the best-fitting models in each mode that we use to compute spectra and likelihoods. The orange stars are the locations of the four points in parameter space sampled for Figs. 4 and 5.

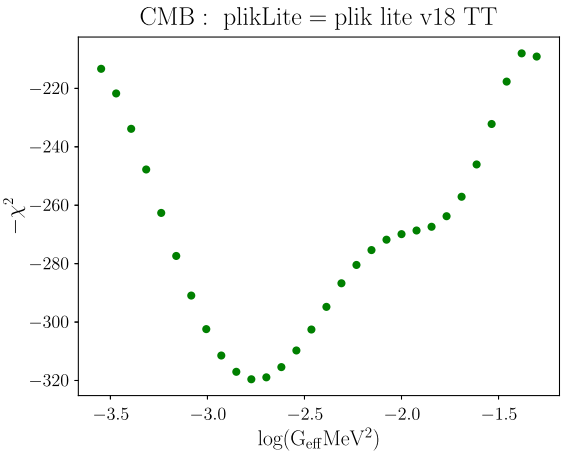

FIG. 3. $-\chi^2$ values for the *Planck* $\ell > 30$ data along the path shown in Fig. 2 to show the clear bimodality and the likelihoods between the two modes. The two modes have the same likelihood; the difference in posterior distribution for $G_{\rm eff}$ is then due to the volume of well-fitting models in our chosen parametrization.

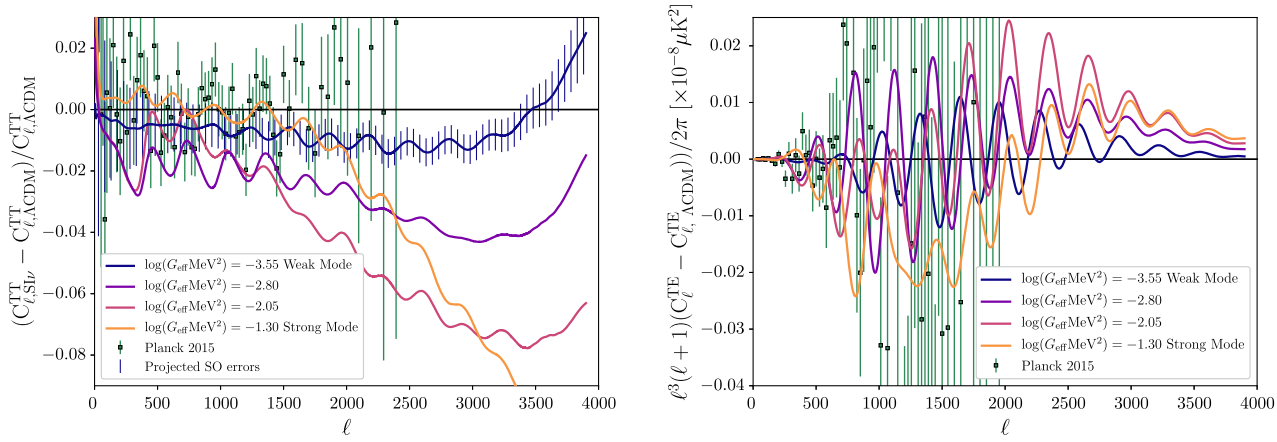

FIG. 4. CMB power spectra (for TT, left, and TE, right) at the points shown in Fig. 2, shown as residuals compared to the best-fitting ΛCDM model from [9]. The *Planck* error bars are shown, and forecasted SO errors are indicated on the left-hand plot. The weak and strong modes both fit $\ell < 2000$ data but diverge at smaller scales and differ in TE. The intermediate values for $G_{\rm eff}$ have a lower TT power at $\ell > 1000$, so are excluded by *Planck* data.

This is at $\log_{10}(G_{\rm eff}{\rm MeV}^2) \approx -2.75$, at which $-\chi^2$ is about 100 lower than at the two peaks. There is a curved path between the two peaks that has a more modest reduction in likelihood: the point at which the two modes have most overlap is displaced from the line that directly connects the peaks in nine-dimensional space. We also find that the low-ℓ CMB temperature, the CMB lensing and the BAO $-\chi^2$ are roughly constant along the path shown in Fig. 2. It is the high-ℓ CMB data that exclude the central region and create the bimodality.

Using Multinest's [55] mode separation algorithm, we calculated the Bayes factor for the two modes, $\mathcal{B} \equiv \frac{\Pr(\mathcal{M}_{\rm strong}|\boldsymbol{d})}{\Pr(\mathcal{M}_{\rm weak}|\boldsymbol{d})}$ (where $\mathcal{M}$ is the cosmological model and $\boldsymbol{d}$ the data from Sec. II). $\mathcal{B} > 1$ would mean the data prefer the strong mode, and $\mathcal{B} < 1$ the weak mode. We find $\mathcal{B} = 0.21 \pm 0.06$, with a ratio of the likelihoods of the peaks of the two modes, $\mathcal{R} \equiv \frac{\max \mathcal{L}(\theta_{\rm strong}|\boldsymbol{d})}{\max \mathcal{L}(\theta_{\rm weak}|\boldsymbol{d})}$, where θ is a set of cosmological parameters, of $R = 1.00$. This indicates that the data prefer $\mathcal{M}_{\rm weak}$ but there are models in $\mathcal{M}_{\rm strong}$ that are as likely as those in $\mathcal{M}_{\rm weak}$ [45,46].

In Fig. 4 we show the TT, and TE spectra for these four models with increasing $G_{\rm eff}$, showing the fractional residual between the spectra and the best-fitting ΛCDM model. Since *Planck* provides a good measurement up to $\ell \approx 2000$, the two modes fit the data well and do not show significant residuals in TT or TE. In contrast, the power spectra corresponding to points in parameter space between the two modes that a reasonable fit to WMAP data as seen in Fig. 1 do not fit the *Planck* TT data at $\ell > 1000$, ℓ range similar to that of WMAP.

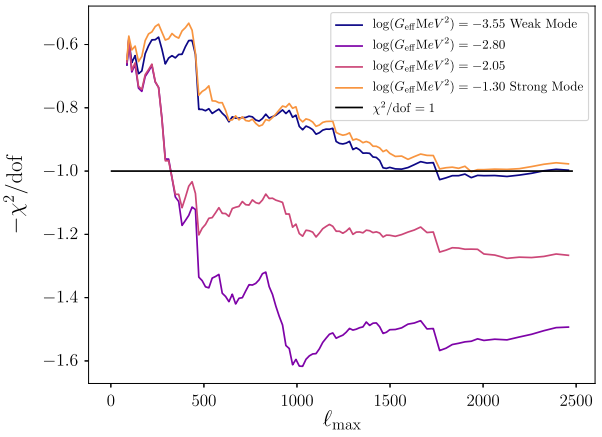

FIG. 5. The goodness of fit ($-\chi^2$/d.o.f. for $\ell > 30$ from the PLIK-LITE *Planck* likelihood) as a function of $\ell_{\rm max}$ for the models shown in Fig. 4. This shows how models between the two well-fitting modes are poor fits to the *Planck* data at small scales.

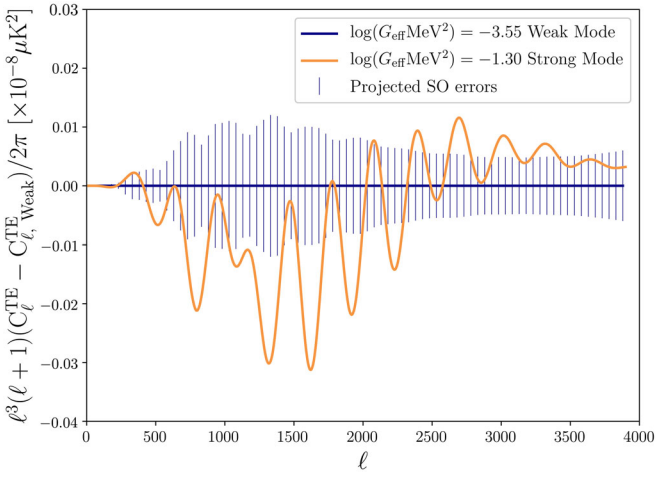

FIG. 6. The residual TE power spectrum between the strong and the weak best-fitting mode, together with the Simons Observatory projected errors. These data should allow the two models to be distinguished.

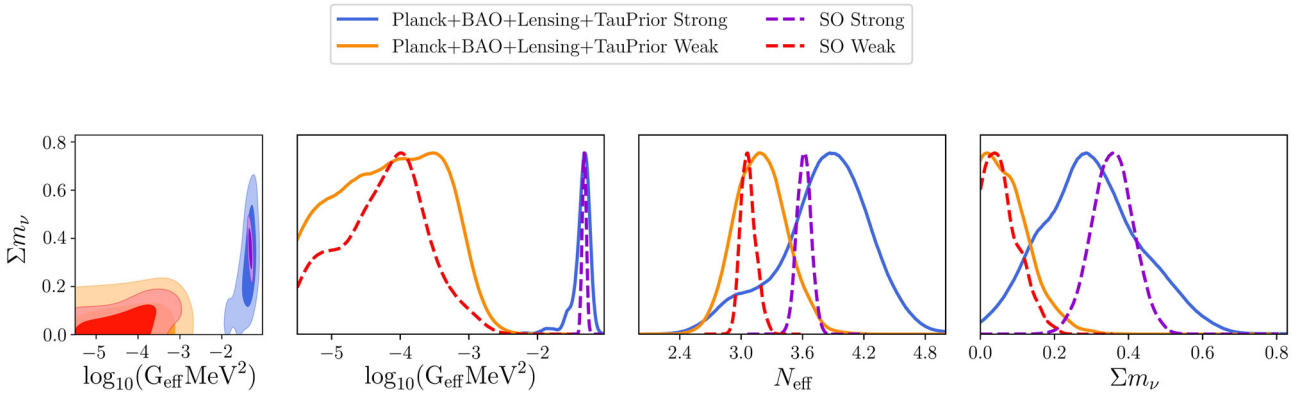

FIG. 7. Forecasted parameter constraints using expected Simons Observatory power spectrum measurements. We forecast for the two modes independently by searching in the parameter space assuming a cosmology described by one of the modes, then swapping the assumed cosmology for the other mode. The distributions are expected to tighten considerably compared to current *Planck* data, and should allow the models to be distinguished.

We examine this scale dependence in more detail by calculating how the $-\chi^2/\text{d.o.f.}$, $-\chi^2$ per degree of freedom (d.o.f.), depends on the smallest scale included, $\ell_{\rm max}$, as shown in Fig. 5. The PLIK-LITE likelihood with $\ell > 30$ follows a Gaussian distribution and permits meaningful d.o.f. counting. We note that the relative shape and difference between the curves, rather than their absolute magnitudes, demonstrates the constraining power as a function of scale. There are significant drops for the two intermediary points around $\ell_{\rm max} \approx 500$ and 1000. With these two drops, the $-\chi^2/\text{d.o.f.}$ of those two points are at $\approx -1.2, -1.5$ respectively, greatly reducing their viability. Meanwhile, the two peaks steadily approach $-\chi^2/\text{d.o.f.} \approx -1$. This is an additional illustration that the $\ell > 1000$ data prefer the two modes but disfavor intermediate interaction strengths.

C. Impact of upcoming CMB data

We explore how upcoming data from the Simons Observatory (SO) will affect the bimodality. Since the posterior is bimodal, we generate two different simulated models.[2] One simulated power spectrum is generated with the best-fitting weak mode power spectra, the other with the best-fitting strong mode power spectra, shown in Fig. 4.

Figure 4 shows that at smaller scales than measured by *Planck*, the two modes diverge from each other. Including the forecasted SO uncertainties, we find that the strong mode differs from the weak mode by more than 1-sigma at $\ell > 2000$. This suggests that with improved small-scale data, we could potentially rule out one of the modes. Furthermore, the two modes also have significantly different TE spectra. We show forecasted SO uncertainties on the weak mode in Fig. 6, finding that the strong mode differs from the weak mode by more than 1σ at most minima. This indicates that the improved TE spectrum's sensitivity to the phase of the CMB power spectrum will help put further constraints on the bimodality.

The forecasted distributions for SO are shown in Fig. 7. The distributions are narrowed significantly compared to those shown in Fig. 1 for *Planck*, suggesting that SO data will be capable of further constraining the parameters for each mode. Indeed, the forecasted constraints on neutrino physics in the weak mode tighten compared to the distributions in Fig. 1 such that the upper bound of $\log_{10}(G_{\rm eff}{\rm MeV}^2)$ decreases, the upper bound of $\sum m_\nu$ decreases by 20%, and the errors on $N_{\rm eff}$ decrease by about 70%. For the strong mode, the errors decrease by about 80% for $\log_{10}(G_{\rm eff}{\rm MeV}^2)$, by about 60% for $\sum m_\nu$, and by 85% for $N_{\rm eff}$.

In each case, for either the strong or weak mode as the input model, the Multinest's mode separation algorithm [55] does not detect the other mode. In fact, the other mode is excluded by many standard deviations. So, if SO finds the data to be significantly closer to one mode than the other, the data would exclude the nonfavored mode.

This is expected as SO will better measure the high ℓTT data, and provide an improved measurement of the TE power spectrum data as shown in Figs. 4 and 6, which are the areas of CMB power spectra data where the two models are nondegenerate. If the true model is ΛCDM, the forecasted uncertainties are small enough to be able to rule out the strong mode. In contrast, if the true model is the best-fitting strongly interacting mode, SO could potentially rule out ΛCDM.

IV. CONCLUSION

By comparing the probability distributions in the parameter space using WMAP and *Planck* data we show that the *Planck* data in the angular range $1000 < \ell < 2500$ allow a model with strongly interacting neutrinos, and disfavor a

[2]Simulated data are produced using the MAKEPERFECTFORECAST.PY code within CosmoMC.

model with more moderate interactions. We explore this in more detail by looking at the power spectra and at the likelihood of the data for increasing $G_{\rm eff}$. We highlight that high ℓTT, and improved TE data will be pivotal in constraining or ruling out the bimodality. The Simons Observatory will make these measurements and is forecasted to significantly improve constraints. If the data were to favor it, SO would be capable of ruling out the bimodality. The strong mode has cosmological parameters that are significantly different to ΛCDM, including a higher Hubble constant, lower amplitude of structure, higher neutrino mass and higher effective neutrino species. While the particular model considered here is *ad hoc*, further exploration of physical models for the neutrino sector seems warranted.

ACKNOWLEDGMENTS

We thank David Spergel and Lyman Page for useful comments and Olivier Doré for early comments. M. P. acknowledges the support of the Department of Astrophysical Sciences at Princeton University. M. P. acknowledges the Hewlett Foundation Fund's support. C. D. K. acknowledges support from the National Science Foundation Award No. DGE1656466 at Princeton University. F.-Y. C.-R. acknowledges the support of the National Aeronautical and Space Administration (NASA) ATP Grant No. NNX16AI12G at Harvard University. Part of this research was carried out during the Undergraduate Summer Research Program at the Department of Astrophysical Sciences, Princeton University.

[1] Q. R. Ahmad *et al.* (SNO Collaboration), Phys. Rev. Lett. **87**, 071301 (2001).
[2] Y. Fukuda, T. Hayakawa, E. Ichihara, K. Inoue, K. Ishihara, H. Ishino, Y. Itow, T. Kajita, J. Kameda, S. Kasuga *et al.*, Phys. Rev. Lett. **81**, 1562 (1998).
[3] S. Weinberg, Phys. Rev. Lett. **43**, 1566 (1979).
[4] T. Yanagida, Prog. Theor. Phys. **64**, 1103 (1980).
[5] R. N. Mohapatra and G. Senjanovic, Phys. Rev. Lett. **44**, 912 (1980).
[6] J. Schechter and J. W. F. Valle, Phys. Rev. D **22**, 2227 (1980).
[7] R. H. Cyburt, B. D. Fields, K. A. Olive, and T.-H. Yeh, Rev. Mod. Phys. **88**, 015004 (2016).
[8] S. Bashinsky and U. Seljak, Phys. Rev. D **69**, 083002 (2004).
[9] N. Aghanim, Y. Akrami, M. Ashdown, J. Aumont, C. Baccigalupi, M. Ballardini, A. Banday, R. Barreiro, N. Bartolo, S. Basak *et al.*, arXiv:1807.06209.
[10] G. Mangano, G. Miele, S. Pastor, T. Pinto, O. Pisanti, and P. D. Serpico, Nucl. Phys. **B729**, 221 (2005).
[11] Z. Bialynicka-Birula, Nuovo Cimento **33**, 1484 (1964).
[12] D. Y. Bardin, S. M. Bilenky, and B. Pontecorvo, Phys. Lett. **32B**, 121 (1970).
[13] G. Gelmini and M. Roncadelli, Phys. Lett. **99B**, 411 (1981).
[14] Y. Chikashige, R. N. Mohapatra, and R. Peccei, Phys. Rev. Lett. **45**, 1926 (1980).
[15] V. D. Barger, W.-Y. Keung, and S. Pakvasa, Phys. Rev. D **25**, 907 (1982).
[16] G. Raffelt and J. Silk, Phys. Lett. B **192**, 65 (1987).
[17] E. W. Kolb and M. S. Turner, Phys. Rev. D **36**, 2895 (1987).
[18] R. V. Konoplich and M. Yu. Khlopov, Yad. Fiz. **47**, 891 (1988) [Sov. J. Nucl. Phys. **47**, 565 (1988)].
[19] A. V. Berkov, Yu. P. Nikitin, A. L. Sudarikov, and M. Yu. Khlopov, Yad. Fiz. **48**, 779 (1988) [Sov. J. Nucl. Phys. **48**, 497 (1988)].
[20] K. M. Belotsky, A. L. Sudarikov, and M. Yu. Khlopov, Yad. Fiz. **64**, 1718 (2001) [Phys. At. Nucl. **64**, 1637 (2001)].
[21] S. Hannestad, J. Cosmol. Astropart. Phys. 02 (2005) 011.
[22] Z. Chacko, L. J. Hall, S. J. Oliver, and M. Perelstein, Phys. Rev. Lett. **94**, 111801 (2005).
[23] S. Hannestad and G. Raffelt, Phys. Rev. D **72**, 103514 (2005).
[24] R. F. Sawyer, Phys. Rev. D **74**, 043527 (2006).
[25] G. Mangano, A. Melchiorri, P. Serra, A. Cooray, and M. Kamionkowski, Phys. Rev. D **74**, 043517 (2006).
[26] A. Friedland, K. M. Zurek, and S. Bashinsky, arXiv: 0704.3271.
[27] D. Hooper, Phys. Rev. D **75**, 123001 (2007).
[28] P. Serra, F. Zalamea, A. Cooray, G. Mangano, and A. Melchiorri, Phys. Rev. D **81**, 043507 (2010).
[29] L. G. van den Aarssen, T. Bringmann, and C. Pfrommer, Phys. Rev. Lett. **109**, 231301 (2012).
[30] K. S. Jeong and F. Takahashi, Phys. Lett. B **725**, 134 (2013).
[31] R. Laha, B. Dasgupta, and J. F. Beacom, Phys. Rev. D **89**, 093025 (2014).
[32] M. Archidiacono, S. Hannestad, R. S. Hansen, and T. Tram, Phys. Rev. D **91**, 065021 (2015).
[33] K. C. Y. Ng and J. F. Beacom, Phys. Rev. D **90**, 065035 (2014).
[34] J. F. Cherry, A. Friedland, and I. M. Shoemaker, arXiv: 1411.1071.
[35] M. Archidiacono, S. Hannestad, R. S. Hansen, and T. Tram, Phys. Rev. D **93**, 045004 (2016).
[36] J. F. Cherry, A. Friedland, and I. M. Shoemaker, arXiv: 1605.06506.
[37] M. Archidiacono, S. Gariazzo, C. Giunti, S. Hannestad, R. Hansen, M. Laveder, and T. Tram, J. Cosmol. Astropart. Phys. 08 (2016) 067.
[38] G. Dvali and L. Funcke, Phys. Rev. D **93**, 113002 (2016).
[39] F. Capozzi, I. M. Shoemaker, and L. Vecchi, J. Cosmol. Astropart. Phys. 07 (2017) 021.
[40] C. Brust, Y. Cui, and K. Sigurdson, J. Cosmol. Astropart. Phys. 08 (2017) 020.
[41] F. Forastieri, Proc. Sci., NOW2016 (**2017**) 084.

[42] O. Balducci, S. Hofmann, and A. Kassiteridis, Phys. Rev. D **98**, 023003 (2018).
[43] C. S. Lorenz, L. Funcke, E. Calabrese, and S. Hannestad, Phys. Rev. D **99**, 023501 (2019).
[44] G. Choi, C.-T. Chiang, and M. LoVerde, J. Cosmol. Astropart. Phys. 06 (2018) 044.
[45] F.-Y. Cyr-Racine and K. Sigurdson, Phys. Rev. D **90**, 123533 (2014).
[46] C. D. Kreisch, F.-Y. Cyr-Racine, and O. Doré, arXiv:1902.00534.
[47] L. Lancaster, F.-Y. Cyr-Racine, L. Knox, and Z. Pan, J. Cosmol. Astropart. Phys. 07 (2017) 033.
[48] M. Archidiacono and S. Hannestad, Astropart. Phys. **7**, 1311 (2014).
[49] I. Oldengott, T. Tram, C. Rampf, and Y. Wong, Astropart. Phys. **11**, 1706 (2017).
[50] G. Barenboim, P. B. Denton, and I. M. Oldengott, Phys. Rev. D **99**, 083515 (2019).
[51] D. Baumann, D. Green, J. Meyers, and B. Wallisch, J. Cosmol. Astropart. Phys. 01 (2016) 007.
[52] A. G. Riess, S. Casertano, W. Yuan, L. Macri, J. Anderson, J. W. MacKenty, J. B. Bowers, K. I. Clubb, A. V. Filippenko, D. O. Jones *et al.*, Astrophys. J. **855**, 136 (2018).
[53] C. Hikage *et al.* (HSC Collaboration), Publ. Astron. Soc. Jpn. **71**, 43 (2019).
[54] A. Lewis and S. Bridle, Phys. Rev. D **66**, 103511 (2002).
[55] F. Feroz and M. P. Hobson, Mon. Not. R. Astron. Soc. **384**, 449 (2008).
[56] Planck Collaboration, Astron. Astrophys. **594**, A11 (2016).
[57] A. Lewis, D. Munshi, P. Ade, N. Aghanim, M. Arnaud, M. Ashdown, J. Aumont, C. Baccigalupi, A. Banday *et al.* (Planck Collaboration), Astron. Astrophys. **594**, A15 (2016).
[58] F. Beutler, C. Blake, M. Colless, D. H. Jones, L. Staveley-Smith, L. Campbell, Q. Parker, W. Saunders, and F. Watson, Mon. Not. R. Astron. Soc. **416**, 3017 (2011).
[59] L. Anderson *et al.*, Mon. Not. R. Astron. Soc. **441**, 24 (2014).
[60] A. J. Ross, L. Samushia, C. Howlett, W. J. Percival, A. Burden, and M. Manera, Mon. Not. R. Astron. Soc. **449**, 835 (2015).
[61] C. L. Bennett *et al.* (WMAP Collaboration), Astrophys. J. Suppl. Ser. **208**, 20 (2013).
[62] J. Aguirre *et al.* (Simons Observatory Collaboration), J. Cosmol. Astropart. Phys. 02 (2019) 056.